

# Multifractal detrended cross-correlation analysis between respiratory diseases and haze in South Korea

Jian Wang<sup>a</sup>, Wei Shao<sup>b</sup>, Junseok Kim<sup>c,\*</sup>

<sup>a</sup>School of Mathematics and Statistics, Nanjing University of Information Science and Technology, Nanjing, 210044, China

<sup>b</sup>Department of Economics, Korea University, Seoul 02841, Republic of Korea

<sup>c</sup>Department of Mathematics, Korea University, Seoul 02841, Republic of Korea

## ARTICLE INFO

### Article history:

Received 20 November 2019

Revised 6 February 2020

Accepted 25 March 2020

Available online 8 April 2020

### Keywords:

$PM_{10}$   
Bronchitis  
Rhinitis  
Multifractality  
Cross-correlation

## ABSTRACT

Recently, air pollution such as the respirable particulate  $PM_{10}$  results in negative impact on human health. We study the non-linear cross-correlations between respiratory diseases and haze in South Korea, using multifractal detrended cross-correlation analysis (MF-DCCA). The empirical tests indicate that there exists cross-correlations between the monthly average  $PM_{10}$ /Bronchitis time series pair, and monthly average  $PM_{10}$ /Rhinitis time series pair. Metrics such as Hurst exponents, scaling exponents, and multifractal spectrums show that the multifractal characteristics of both the time series pairs are significant. In addition, we compare the degrees of multifractal spectrums and find that the cross-correlation of the time series pair  $PM_{10}$ /Bronchitis is stronger than that of  $PM_{10}$ /Rhinitis, which indicates that the monthly outpatient quantity of bronchitis is more sensitive to  $PM_{10}$  concentration. Furthermore, to identify the main source of multifractality for two time series pairs, we phase-randomize and shuffle the original series. The computational results demonstrate that fat-tailed distribution contributes to the multifractality between respiratory diseases and haze.

© 2020 Elsevier Ltd. All rights reserved.

## 1. Introduction

Recently, with the advent of modernization and urbanization, environmental damage and air pollution have been caused at the same time of economic development. More and more evidence has suggested that there exists impact of air pollution on human health, especially for human respiratory system. Among numerous air pollutants, particulate matter (PM) has drawn great attention, and research showed that the PMs with aerodynamic diameter less than 10 microns has a greater impact on human respiratory system.

It was found that for every  $10 \mu\text{g}/\text{m}^3$  of  $PM_{10}$  increased, the mortality of respiratory system increased by 0.58%, after investigating 29 European cities [1]. A recent review [2] showed that the deposition of  $PM_{2.5}$  particles in the acinar area of the lung is uneven by a high-resolution fluorescence imaging method, and the maximum deposition rate in the acinar region is remarkably different from the prediction of the average deposition model, and the deposition of these particles in the lung is harmful to human health. Moreover, many studies have reported the effects of atmospheric particles on mortality induced by respiratory diseases. Pope et al.

[3] investigated the relationship between long-term PMs exposure and mortality, and the relationship between PMs and mortality patterns and specific sources of death. The results indicated that long-term PMs exposure was closely related to the mortality of ischemic heart disease. For these cardiovascular causes of death, an increase of  $10 \mu\text{g}/\text{m}^3$  in fine particles was associated with an increased risk of mortality of 8% to 18%, the risk of smokers was comparable or greater than that of non-smokers, and the correlation between mortality and respiratory diseases was relatively weak. Atkinson et al. [4] found that  $10 \mu\text{g}/\text{m}^3$  increase in  $PM_{2.5}$  was associated with a 1.04% increase in the risk of death, and there are significant regional differences (0.25%–2.08%) in worldwide.

In South Korea, haze caused by atmospheric particles has recently become more and more serious. In some previous works, there have been studies on the relationship between air pollution and respiratory system in South Korea. Kwon et al. [5] studied the mortality from  $PM_{10}$  exposure in Seoul, and found the mortality increased by 4.1% due to respiratory and cardiovascular causes. According to Jun et al. [6], they suspected that when air quality deteriorates, people have a stronger incentive to adapt to it in behavior, and their results implied that in polluted areas, the possibility of respiratory diseases decreases with the gradual increase of air pollution, which can be interpreted by behavioral adaptation to the environment, while in particularly polluted areas, the effectiveness of such adaptation seems limited. Kim et al. [7] es-

\* Corresponding author.

E-mail address: [cfdkim@korea.ac.kr](mailto:cfdkim@korea.ac.kr) (J. Kim).

URL: <http://math.korea.ac.kr/~cfdkim/> (J. Kim)

timated the impact of  $PM_{10}$  on health in Seoul, South Korea, between 2014 and 2015, and found a significant correlation between the MODerate-resolution Imaging Spectroradiometer Aerosol Optical Depth (MODIS AOD) and  $PM_{10}$  concentration, in particular, during winter season.

However, no researchers have used the method of multifractal detrended cross-correlation analysis (MF-DCCA) to discuss the cross-correlation between  $PM_{10}$  exposure and the number of outpatients with respiratory diseases. In this study, in order to explore the impact of  $PM_{10}$  concentration on people's health in South Korea, and to provide scientific basis for taking positive response strategies and interventions, we study the relationship between  $PM_{10}$  in air pollutants in South Korea and the number of outpatients with respiratory diseases in hospitals, using MF-DCCA, which has been proved to be an effective tool for analyzing the correlations between two time series, and it was first proposed by Zhou [8]. Afterwards, MF-DCCA has been used in many fields such as financial markets [9–11], traffic flow [12], and the cross-correlations between  $PM_{2.5}$  and meteorological factors [13]. Recently, Wang et al. [14] used MF-DCCA to investigate the cross-correlations between meteorological factors and bacterial foodborne diseases.

In this paper, we adopted three parameter variables, such as the monthly average concentration of  $PM_{10}$ , the monthly average outpatient quantity of bronchitis, and the monthly average outpatient quantity of rhinitis, in the whole South Korea from January 2010 to March 2019.

The paper is organized in the following manner. Section 2 briefly introduces the method. Section 3 describes the data sources. Section 4 presents computational results. Conclusions are provided in the last section.

## 2. Principles and methodology

### 2.1. Multifractal detrended cross-correlation analysis

The multifractal detrended fluctuation analysis (MF-DFA) has been proved to be an effective way that can measure the multifractal properties of non-stationary time series [15–22]. To investigate the correlations of two non-stationary time series, Podobnik et al. [23] proposed DCCA method. MF-DCCA method was proposed to study the multifractal characteristics of two non-stationary time series by Zhou [8]. In this work, we check the correlations between  $PM_{10}$  concentration and outpatient quantity of respiratory diseases time series using MF-DCCA. The process of MF-DCCA is generally described as follows.

I. Given two time series  $\{x_t, y_t, t = 1, 2, \dots, N\}$ ,  $N$  is the length of time series. Next, create the cumulative deviation series.

$$X(t) = \sum_{k=1}^t (x_k - \bar{x}), \quad t = 1, 2, \dots, N, \quad (1)$$

$$Y(t) = \sum_{k=1}^t (y_k - \bar{y}), \quad t = 1, 2, \dots, N, \quad (2)$$

where  $\bar{x}$  and  $\bar{y}$  denote the mean of the time series  $x_t$  and  $y_t$ .

II. Divide the cumulative deviation series  $X$  and  $Y$  into  $N_s = \text{int}(\frac{N}{s})$  non-overlapping segments, where  $s$  is the time scale. If  $N$  is not an integral multiple of  $s$ , some information will be left at the end of the series. To include all the information of the time series, the same procedure is repeated from the end to the start. Via taking this step, then  $2N_s$  non-overlapping segments are obtained.

III. For each subsegment  $v$ , we use least squares method to acquire the local trends with an  $k$ th-order polynomial fit.

$$x_v(i) = a_1 i^k + a_2 i^{k-1} + \dots + a_k i + a_{k+1}, \quad (3)$$

$$i = 1, 2, \dots, s; \quad k = 1, 2, \dots$$

$$y_v(i) = b_1 i^k + b_2 i^{k-1} + \dots + b_k i + b_{k+1}, \quad (4)$$

$$i = 1, 2, \dots, s; \quad k = 1, 2, \dots$$

IV. Calculate the detrended covariance  $F^2(s, v)$ . When  $v = 1, 2, \dots, N_s$ ,

$$F^2(s, v) = \frac{1}{s} \sum_{i=1}^s \{ |X[(v-1)s+i] - x_v(i)| |Y[(v-1)s+i] - y_v(i)| \}. \quad (5)$$

When  $v = N_s + 1, N_s + 2, \dots, 2N_s$ ,

$$F^2(s, v) = \frac{1}{s} \sum_{i=1}^s \{ |X[N - (v - N_s)s + i] - x_v(i)| |Y[N - (v - N_s)s + i] - y_v(i)| \}. \quad (6)$$

V. Averaging the detrended covariances to obtain the  $q$ th-order wave function as

$$F_q(s) = \left\{ \frac{1}{2N_s} \sum_{v=1}^{2N_s} [F^2(s, v)]^q \right\}^{\frac{1}{q}}. \quad (7)$$

When  $q = 0$ , according to Lopida's law,

$$F_q(s) = \exp \left( \frac{1}{2N_s} \sum_{v=1}^{2N_s} \ln[F^2(s, v)] \right). \quad (8)$$

If scaling behavior do exist, then the power-law correlations satisfy  $F_q(s) \propto s^{h_{xy}(q)}$ .  $h_{xy}(q)$  is the generalized Hurst exponent versus  $q$ , the extent of multifractality can be derived by calculating the range of  $h_{xy}(q)$ , a larger  $\Delta h_{xy} = h_{xy}(q_{\min}) - h_{xy}(q_{\max})$  means stronger multifractal feature.

If  $q = 2$ , the MF-DCCA becomes the DCCA, if  $h_{xy}(2) = 0.5$ , it indicates the two time series have no cross-correlations with each other, when  $h_{xy}(2) > 0.5$ , the cross-correlations are positive persistent, when  $h_{xy}(2) < 0.5$ , the cross-correlations are anti-persistent.

### 2.2. Mass exponent and multifractal spectrum

Let us define the mass exponent spectrum  $\tau_{xy}(q)$  as

$$\tau_{xy}(q) = q h_{xy}(q) - 1, \quad (9)$$

where  $h_{xy}(q)$  is obtained from MF-DCCA. The singularity strength  $\alpha_{xy}$ , which describes the singular degree of each segment in a complex system; and the singularity spectrum  $f_{xy}(\alpha)$ , which describes fractal dimension of  $\alpha_{xy}$  are obtained from

$$\alpha = h_{xy}(q) + q h'_{xy}(q), \quad (10)$$

$$f_{xy}(\alpha) = q[\alpha_{xy} - h_{xy}(q)] + 1. \quad (11)$$

The range of the singularity strength  $\Delta \alpha_{xy} = \alpha_{xy_{\max}} - \alpha_{xy_{\min}}$  determine the strength of multifractality. According to [24], a larger  $\Delta \alpha_{xy}$  indicates a more intense data fluctuation.

## 3. Data collection

We use monthly average time series of  $PM_{10}$  ( $\mu\text{g}/\text{m}^3$ ) concentration, outpatient quantity of bronchitis, and outpatient quantity of rhinitis data to study the cross-correlation between air pollution and respiratory diseases. The experimental samples for bronchitis data and rhinitis data are downloaded from "Health Insurance Review and Assessment Service", please refer to website: <http://opendata.hira.or.kr/op/opc/olapMfrnIntrsIlnsInfo.do>. The source data of  $PM_{10}$  concentrations are obtained from "Korea Environment Corporation", and specific data are provided by the monitoring station of Jung gu, Seoul. The detailed information can be

**Table 1**  
Descriptive statistics.

Category	Minimum	Maximum	Mean	Standard deviation	Skewness	Kurtosis
PM <sub>10</sub>	19	85	44.4685	13.6833	0.3238	2.6767
Bronchitis	73	2760	823	548	1.1175	3.7775
Rhinitis	32,081	116,621	74,267	21,078	-0.1656	2.1553

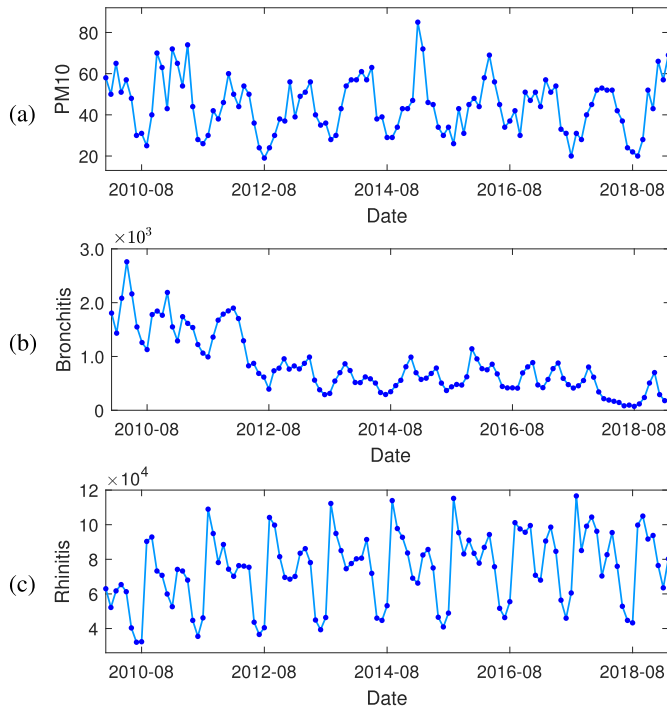


**Fig. 1.** Monthly average time series of (a) PM<sub>10</sub> concentration, (b) outpatient quantity of bronchitis, and (c) outpatient quantity of rhinitis.

downloaded from website: <https://www.airkorea.or.kr>. The selection of time interval is from January 2010 to March 2019, and each category includes 111 samples. The descriptive statistics for each time series are listed in Table 1.

The time series charts for the changing trend of PM<sub>10</sub> concentration, outpatient quantity of bronchitis, and outpatient quantity of rhinitis data are shown in Fig. 1. From Fig. 1(b) and (c), we can observe clearly that there are more outpatient quantity of both bronchitis and rhinitis during winter than during summer months.

#### 4. Experiment results

For the empirical research, the first step is to select appropriate parameters, then conduct the tests for each single time series using MF-DFA. Then cross-correlation test function and DCCA coefficient are applied to test the correlations between PM<sub>10</sub> concentration and outpatient quantity of respiratory diseases. At last, we adopt MF-DCCA to study the cross-correlations from the perspective of quantity. Meanwhile, we investigate the main causes of multifractality of each series pair. It is suggested by [25] that polynomial order  $k$  can be selected from 1 to 3. In this article, we take  $k = 2$  to prevent polynomial over-fitting or under-fitting. By [26,27], when studying the multifractality of PM<sub>10</sub>, the segment size can be considerably stay from 4 to the value of 1/4 of the sample size. In this study, the minimum and maximum segment scales are selected as  $s_{\min} = 10$  and  $s_{\max} = 20$ , respectively. Lashermes et al. [28] suggests that  $q$  can be chosen from  $-10$  to  $10$ .

**Table 2**  
Multifractality of PM<sub>10</sub>, bronchitis, and rhinitis time series.

	$h(2)$	$\Delta H(q)$	$\Delta\alpha$
<b>PM<sub>10</sub></b>	1.2936	<b>1.1083</b>	<b>1.4315</b>
<b>Bronchitis</b>	1.1087	0.8466	1.1058
<b>Rhinitis</b>	0.6960	0.8873	1.2091

#### 4.1. Preliminary test on multifractality

We first apply MF-DFA to investigate the multifractality of three separate time series. We depict the log-log fluctuation function  $F_q(s)$  versus fractal order  $q$  based on a varied  $s$  for PM<sub>10</sub>, bronchitis, and rhinitis in Fig. 2. We observe that for each series, lines from  $q = -10$  to  $q = 10$  can fit the curve of fluctuation functions well, indicating the power-law behavior and long-range correlations exist for each series, from the bottom to the top are  $q = -10$ ,  $q = -6$ ,  $q = -2$ ,  $q = 2$ ,  $q = 6$ , and  $q = 10$ , respectively. The decreasing slope with the increasing of  $q$  indicates that all the time series display a multifractal behavior.

To compute the multifractality quantitatively, we first calculate  $h(q)$  with  $q$  from  $-10$  to  $10$ . The Hurst exponents of  $h(q) - q$  for the three schemes are shown in Fig. 3.

As shown in Fig. 3, we see that the generalized Hurst exponents for three time series are not fixed values, and  $h(q)$  decrease with the increase of  $q$ , which shows that the time series of PM<sub>10</sub>, bronchitis, and rhinitis exist multifractal properties. We note that when  $q = 2$ ,  $h(2)$  of all the time series are greater than 0.5, all the  $h(2)$  values are listed in Table 2. In addition, the wavelet fluctuations of all the time series have significant persistence, since we observe the value of  $h(q)$  decreases rapidly with the increasing of  $q$  when  $q < 0$ . While  $q > 0$ , all the time series behave the minimum sustainability of large fluctuations, as we can see  $h(q)$  stays slightly when  $q$  increases. From these Hurst exponents, let the degree of multifractality be defined by

$$\Delta H(q) = h(q_{\min}) - h(q_{\max}). \tag{12}$$

The values of  $\Delta H$  for each single time series are shown in Table 2.

Research [29] showed that curvature of scaling exponent can measure the multifractality. The scaling exponents  $\tau(q)$  are estimated by Eq. (9). In Fig. 4, the scaling exponents of three time series are non-linearly dependent on  $q$ , which shows another evidence of multifractality.

Then, we calculate multifractal spectrum. From Fig. 5, the widths of multifractal spectra for series pairs are significantly nonzero, indicating that all the series are multifractal. We notice the  $\Delta\alpha$  of all the time series, and find the  $\Delta\alpha$  of PM<sub>10</sub> is the largest, which implies the multifractal nature is the strongest. The maximum multifractal strength value for metrics  $\Delta H(q)$  and  $\Delta\alpha$  are highlighted in bold in Table 2.

#### 4.2. Cross-correlation test

Qualitative tests of the cross-correlations between two time series are essential for this study. We first show the correlations between PM<sub>10</sub> concentration and respiratory diseases time series. Assuming that there exists two time series,  $X_t$  and  $Y_t$ ,  $t = 1, 2, \dots, T$ ,

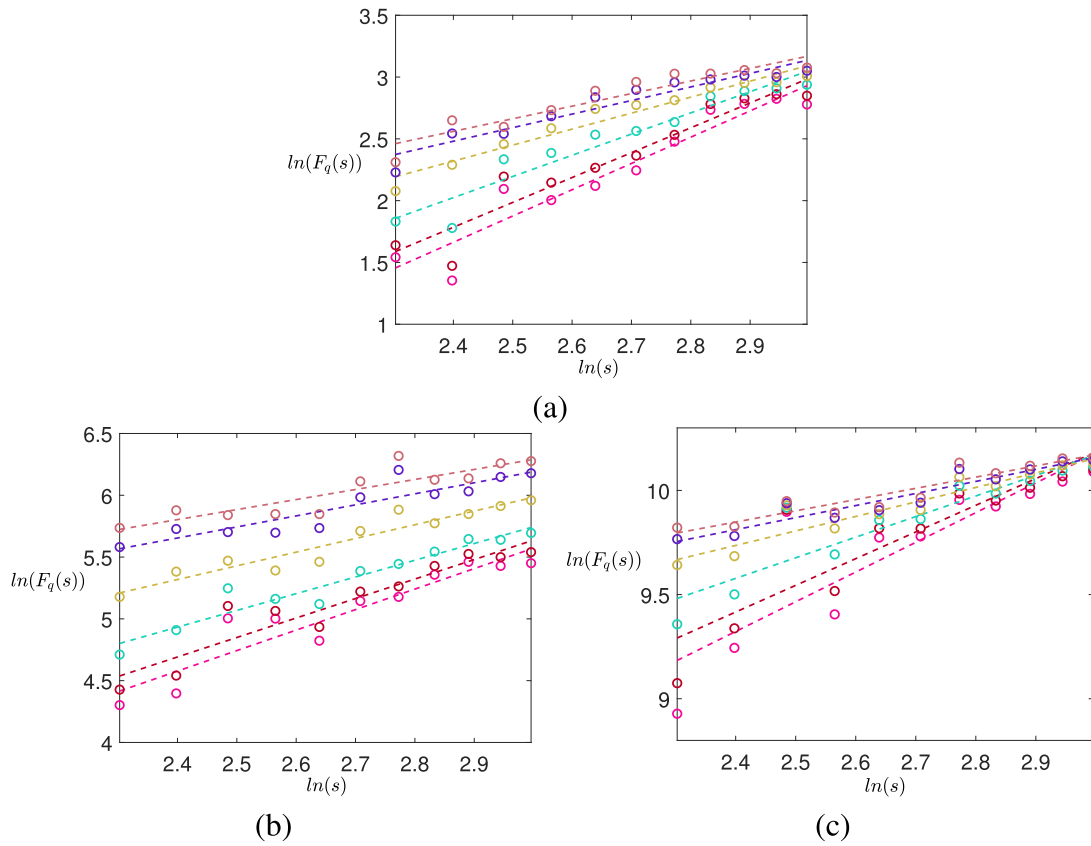


Fig. 2. Loglog plots of fluctuation function  $F_q(s)$  of (a)  $PM_{10}$ , (b) bronchitis, and (c) rhinitis.

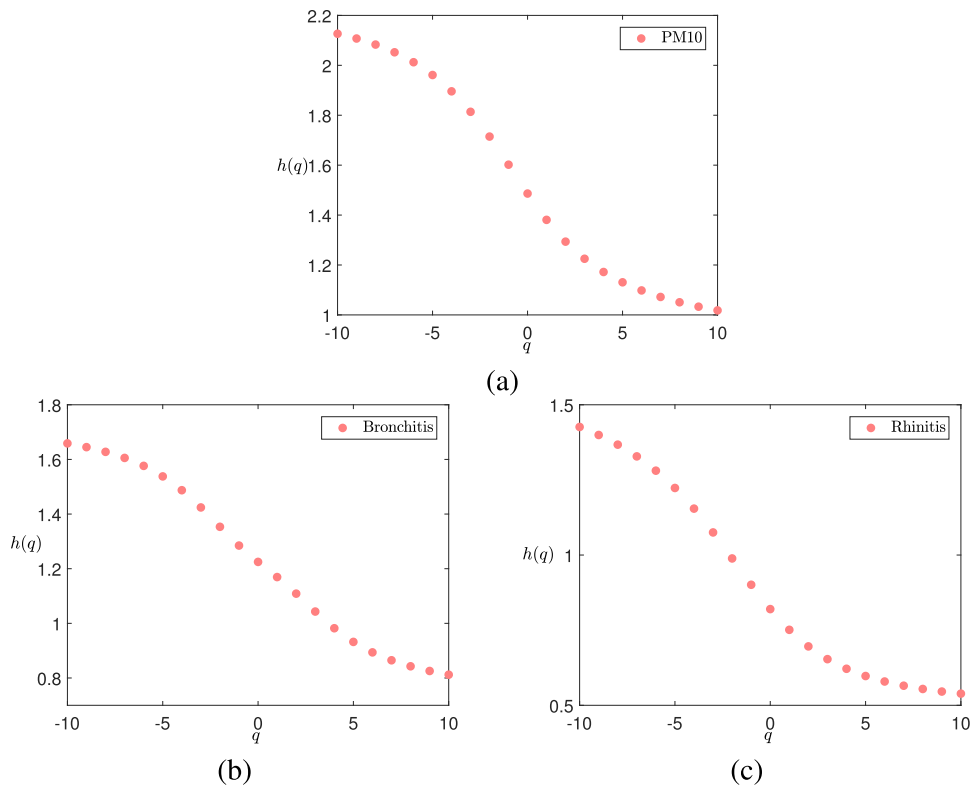


Fig. 3. Generalized Hurst exponents of (a)  $PM_{10}$ , (b) bronchitis, and (c) rhinitis.

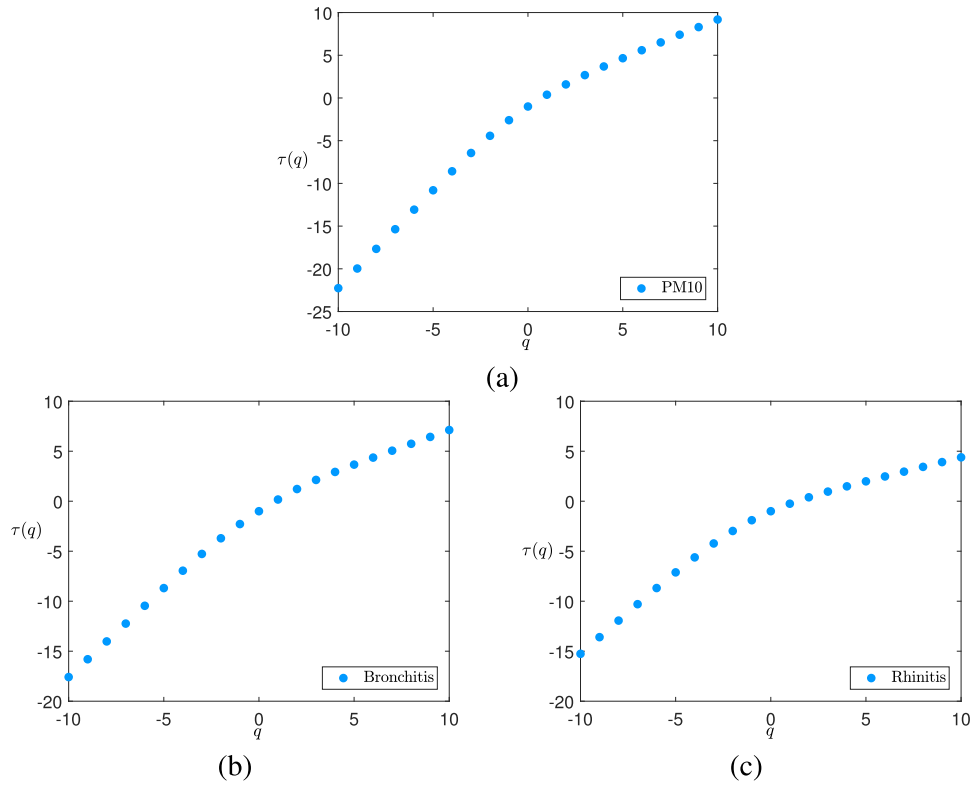


Fig. 4. Scaling exponents of (a)  $PM_{10}$ , (b) bronchitis, and (c) rhinitis.

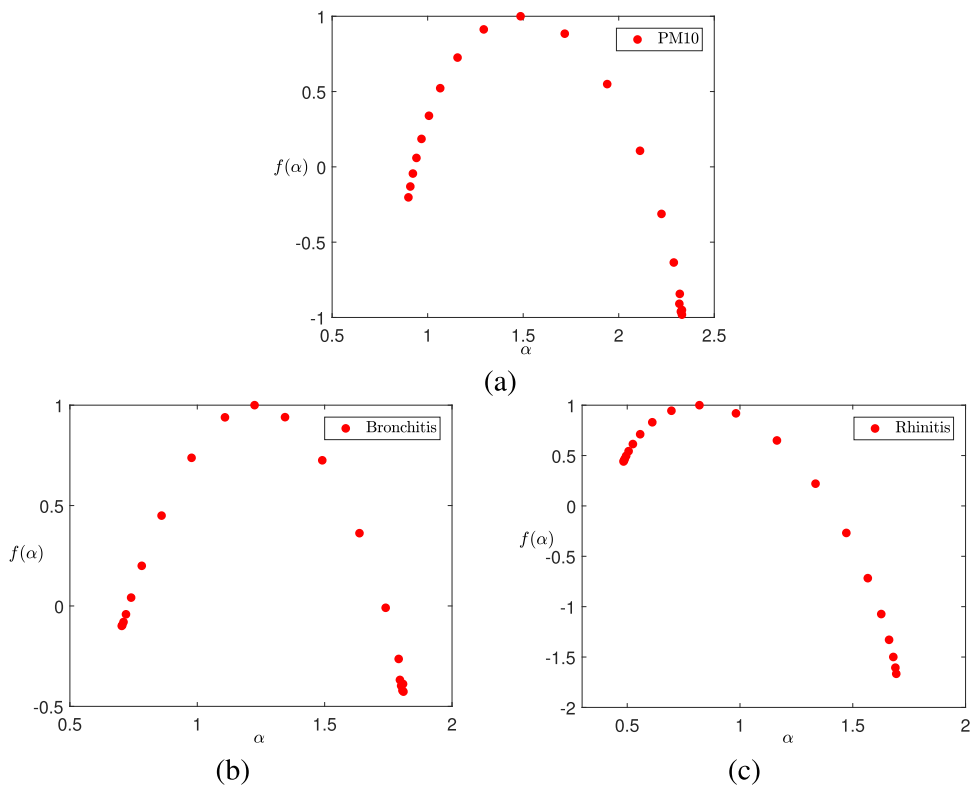


Fig. 5. Multifractal spectrums of (a)  $PM_{10}$ , (b) bronchitis, and (c) rhinitis.

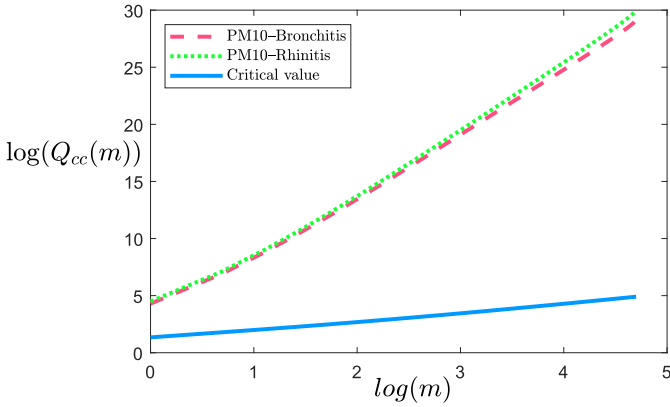


Fig. 6. Cross-correlation test versus  $\log(m)$ . A color version of the figure is available in the web version of the article.

the cross-correlation test function is given by

$$C_i = \frac{\sum_{k=i+1}^T X_k Y_{k-i}}{\sqrt{\sum_{k=1}^T X_k^2 \sum_{k=1}^T Y_k^2}}. \quad (13)$$

Then, we get the test statistic as follows.

$$Q_{cc}(m) = T^2 \sum_{i=1}^m \frac{C_i^2}{T-1}. \quad (14)$$

In this study, the degree of freedom  $m$  varying from 1 to 110, and the critical value is set for  $\chi^2(m)$  distribution at 5% level of significance.

As the cross-correlation statistics for two pairs of indices ( $PM_{10}$ /Bronchitis and  $PM_{10}$ /Rhinitis) shown in Fig. 6, the  $Q_{cc}(m)$  for two time series pairs always go above the critical values as  $m$  increases, implying the statistically significant of long-range cross-correlations between  $PM_{10}$  concentration and respiratory diseases time series. In Fig. 6, the critical value of the cross-correlation statistics is represented by the blue line. The red line denotes the cross-correlation statistic  $Q_{cc}(m)$  of the pair of  $PM_{10}$ /Bronchitis and the green line represents the pair of  $PM_{10}$ /Rhinitis, respectively.

#### 4.3. DCCA coefficient

DCCA coefficient has been an efficient metric to evaluate the highly non-stationary processes since it was proposed by Zebende [30]. DCCA coefficient was also proved to be able to quantify the significance of the correlation between different time series in [31]. In the investigation of agricultural futures market in China and the United States, DCCA coefficient was also used by Li et al. [32] to test the cross-correlations between the series. In this study, we use this method to further test the cross-correlations between  $PM_{10}$ /Bronchitis series pair and  $PM_{10}$ /Rhinitis series pair. The DCCA coefficient function is defined as follows.

$$\rho_{DCCA} = \frac{F_{DCCA_{ab}}^2(s)}{F_{DFA_a}(s)F_{DFA_b}(s)}. \quad (15)$$

$F_{DCCA_{ab}}^2(s)$  is the detrended covariance's fluctuation function of time series pair,  $F_{DFA_a}(s)$  and  $F_{DFA_b}(s)$  represent each single detrended fluctuation function. The value of  $\rho_{DCCA}$  ranges from  $-1$  to  $1$ . A closer value to  $1$  means the series pair has a higher cross-correlation. When  $\rho_{DCCA} = 0$ , there exists no cross-correlation. A closer value to  $-1$  means the cross-correlation of the series pair is more anti-persistent. We plot the DCCA coefficient versus window sizes  $s$  in Fig. 7, where  $s$  varied from 10 to 20.

The red curve denotes the DCCA coefficient between monthly average time series of  $PM_{10}$  concentration and outpatient quan-

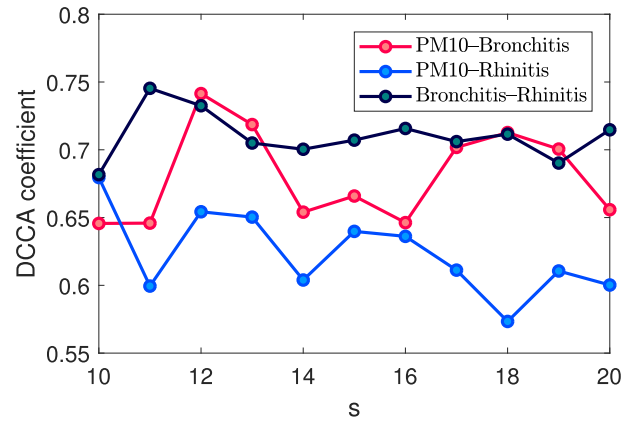


Fig. 7. DCCA coefficients for three time series pairs. A color version of the figure is available in the web version of the article.

tity of bronchitis while the blue curve represents the DCCA coefficient between monthly average time series of  $PM_{10}$  concentration and outpatient quantity of rhinitis, and black curve form the DCCA coefficient of Bronchitis/Rhinitis series pair. We note that all the values are within the interval of 0 to 1, indicating the cross-correlations exist in  $PM_{10}$ /Bronchitis,  $PM_{10}$ /Rhinitis, and Bronchitis/Rhinitis series pairs. From Fig. 7, we observe that the correlations between bronchitis and rhinitis is the largest, then the  $PM_{10}$ /Bronchitis series pair,  $PM_{10}$ /Rhinitis is the lowest.

#### 4.4. MF-DCCA analysis

As the cross-correlation statistics  $Q_{cc}(m)$  and DCCA coefficient show the existence of cross-correlations for two time series pairs, to study the cross-correlations quantitatively, we apply MF-DCCA to further estimate the cross-correlations for time series pairs ( $PM_{10}$ /Bronchitis and  $PM_{10}$ /Rhinitis). Firstly, we show the log-log plots of  $F_q(s)$ . As shown in Fig. 8, the fluctuation values of both  $PM_{10}$ /Bronchitis and  $PM_{10}$ /Rhinitis series pairs increase with segment  $s$ , implying both the two series pairs have long-range correlations. From the bottom to the top are  $q = -10$ ,  $q = -6$ ,  $q = -2$ ,  $q = 2$ ,  $q = 6$ , and  $q = 10$ , respectively. The decreasing slope with the increasing of  $q$  indicates that both the series pairs display a strong multifractal behavior, which refers that both the two monthly outpatient volume of respiratory diseases are sensitive to  $PM_{10}$  concentration, they have strong cross-correlations.

Furthermore, as shown in Table 3 and Fig. 9, the cross-correlation generalized Hurst exponents  $h_{xy}(q)$  of  $PM_{10}$ /Bronchitis and  $PM_{10}$ /Rhinitis series pairs decline with the increase of  $q$ , indicating each series pair possess multifractal property. In addition, when  $q = 2$ , the cross-correlation exponents for both  $PM_{10}$ /Bronchitis and  $PM_{10}$ /Rhinitis series pairs are larger than 0.5, showing both time series pairs have persistence. We list the values of  $h_{xy}(2)$  for two indices in Tables 3 and 4. Moreover, the  $h_{xy}(2)$  value of  $PM_{10}$ /Bronchitis is larger than  $PM_{10}$ /Rhinitis, indicating the cross-correlation of  $PM_{10}$ /Bronchitis series pair is more persistent than  $PM_{10}$ /Rhinitis series pair.

In Fig. 9, we also see that the wavelet fluctuations of all the time series pairs have significant positive persistence, since we observe the value of  $h_{xy}(q)$  decreases rapidly with the increasing of  $q$  when  $q < 0$ . While  $q > 0$ , both the time series pairs behave the minimum sustainability of large fluctuations, as we can see  $h_{xy}(q)$  stays slightly when  $q$  increases. Then, let the degree of multifractality be given by

$$\Delta H_{xy}(q) = h_{xy}(q_{min}) - h_{xy}(q_{max}). \quad (16)$$

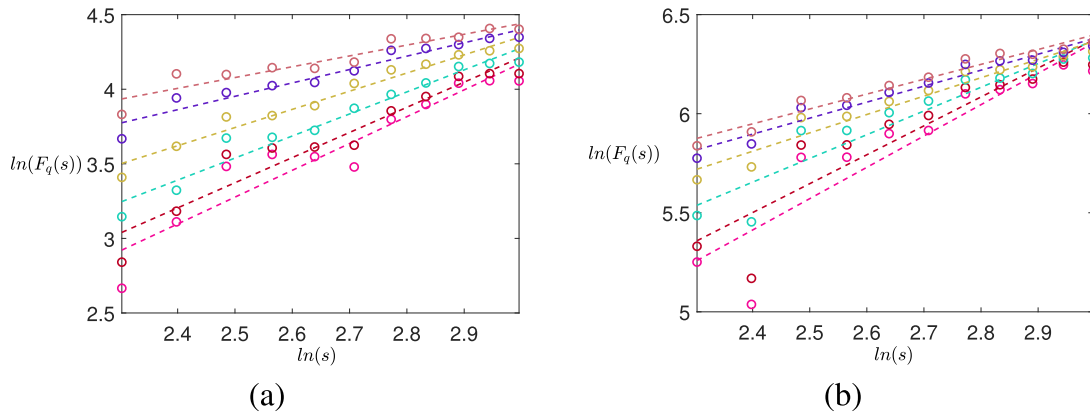


Fig. 8. Loglog plots of fluctuation function  $F_q(s)$  of (a)  $PM_{10}$ /Bronchitis, and (b)  $PM_{10}$ /Rhinitis.

Table 3

Generalized Hurst exponents  $h_{xy}(q)$  of two time series pairs.

q	PM <sub>10</sub> /Bronchitis	PM <sub>10</sub> /Rhinitis
-10	1.7982	1.5814
-9	1.7779	1.5592
-8	1.7532	1.5322
-7	1.7229	1.4993
-6	1.6860	1.4587
-5	1.6415	1.4088
-4	1.5901	1.3480
-3	1.5345	1.2764
-2	1.4781	1.1970
-1	1.4219	1.1163
0	1.3628	1.0421
1	1.2960	0.9790
2	<b>1.2187</b>	<b>0.9278</b>
3	1.1335	0.8869
4	1.0474	0.8543
5	0.9672	0.8281
6	0.8976	0.8067
7	0.8397	0.7889
8	0.7928	0.7741
9	0.7553	0.7614
10	0.7254	0.7505

Table 4

Multifractality for two series pairs of  $PM_{10}$ /Bronchitis and  $PM_{10}$ /Rhinitis.

	$h_{xy}(2)$	$\Delta H_{xy}(q)$	$\Delta\alpha_{xy}$
PM <sub>10</sub> /Bronchitis	1.2187	<b>1.0728</b>	<b>1.5156</b>
PM <sub>10</sub> /Rhinitis	0.9278	0.8309	1.1401

The values of  $\Delta H_{xy}$  for each time series pair are shown in Table 4. We observe that with the increasing of  $q$ , the range of  $h_{xy}(q)$  fluctuation of the time series pair of  $PM_{10}$ /Bronchitis is greater, implying the multifractal feature is greater, that is to say, the monthly outpatient volume of bronchitis is more sensitive to  $PM_{10}$  concentration than that of rhinitis, and the cross-correlation of  $PM_{10}$ /Bronchitis is greater.

In Fig. 10, the scaling exponents  $\tau_{xy}(q)$  of two time series pairs are non-linearly dependent on  $q$ , which shows another evidence of multifractality for both two time series pairs.

At last, we use multifractal strength and spectrums to examine  $PM_{10}$ /Bronchitis and  $PM_{10}$ /Rhinitis time series pairs. As shown in Fig. 11 and Table 4, the widths of multifractal spectra for series pairs are significantly nonzero, indicating that all the series are multifractal. We notice the  $\Delta\alpha_{xy}$  of both two time series pairs, and find the  $\Delta\alpha$  of  $PM_{10}$ /Rhinitis is narrower, which implies the multifractal nature of  $PM_{10}$ /Rhinitis is weaker and the monthly outpa-

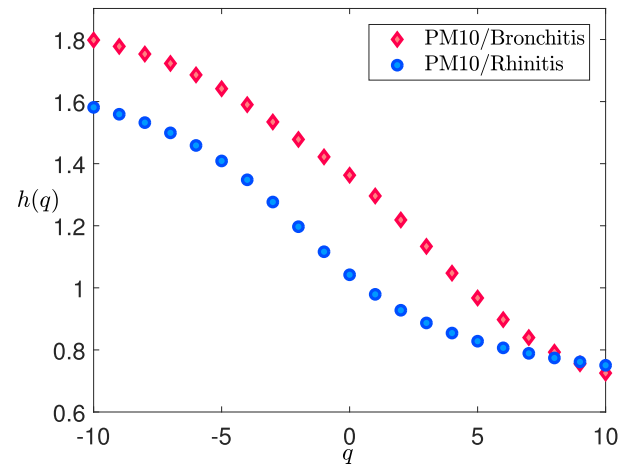


Fig. 9. Generalized Hurst exponents of  $PM_{10}$ /Bronchitis, and  $PM_{10}$ /Rhinitis. A color version of the figure is available in the web version of the article.

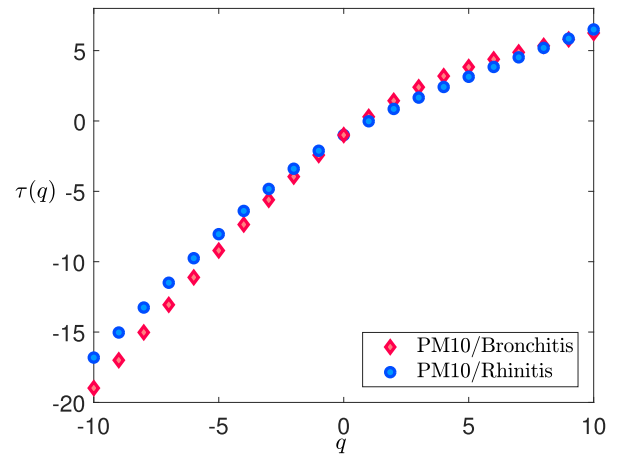


Fig. 10. Scaling exponents of  $PM_{10}$ /Bronchitis, and  $PM_{10}$ /Rhinitis. A color version of the figure is available in the web version of the article.

tient volume of bronchitis is more relevance to  $PM_{10}$  concentration. The maximum multifractal strength value for metrics  $\Delta H_{xy}(q)$  and  $\Delta\alpha_{xy}$  are highlighted in bold in Table 4.

#### 4.5. The sources of multifractal features

According to the former studies [8,15,33], generally, there are two causes of multifractality: (1) long-range correlations, and (2)

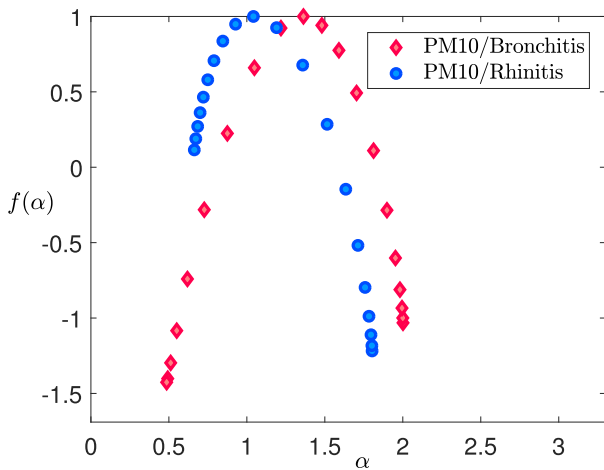


Fig. 11. Multifractal spectrums of  $PM_{10}$ /Bronchitis, and  $PM_{10}$ /Rhinitis. A color version of the figure is available in the web version of the article.

fat-tail distributions. Now, we construct phase-randomized and shuffled time series to explore the main cause of multifractality for each time series pair. The shuffled series can be randomly generated as follows. For a time series with length  $N$ , creating  $(a, b)$  of random integers with  $a, b \leq N$ , then change the value in  $a$ -th order with  $b$ -th order, and repeat the above process for sufficient times. Moreover, for the phase-randomized time series, we first create a series of random numbers with the Gaussian distribution, then arrange the series with the same order.

As same as above procedure, we first calculate the cross-correlations generalized Hurst exponent  $h_{xy}(q)$ , then the  $\tau_{xy}(q)$ , at last the  $\Delta\alpha_{xy}$ . From Figs. 12–14, we note that all the series pairs are strongly multifractal, and  $h_{xy}(2)$  for all shuffled and phase-randomized time series pairs of  $PM_{10}$ /Bronchitis are less than 0.5, showing that there existing negative persistent, and the negative persistent property of phase-randomized is stronger than shuffled time series pair. Besides,  $h_{xy}(2)$  for shuffled time series pair of  $PM_{10}$ /Rhinitis is larger than 0.5, however, much less than the original series pair, it implies that the shuffled series pair become weaker persistent. Moreover, for phase-randomized time series pairs of  $PM_{10}$ /Rhinitis,  $h_{xy}(2)$  is less than 0.5, indicating the series pair has negative persistent property. We list the values of  $h_{xy}(2)$  for original, shuffled, and phase-randomized time series pairs in Table 5. To obtain the robust results, we use the mean of 50 repeated values for shuffled, and phase-randomized time series.

Table 5  
Multifractality of original, shuffled, and phase-randomized series for two series pairs of  $PM_{10}$ /Bronchitis, and (b)  $PM_{10}$ /Rhinitis.

		$h(2)$	$\Delta\alpha$
	Original	1.2187	1.5156
$PM_{10}$ /Bronchitis	Shuffled	0.4786	0.8753
	Phase-randomized	0.3913	<b>0.7764</b>
$PM_{10}$ /Rhinitis	Original	0.9278	1.1401
	Shuffled	0.5562	0.3501
	Phase-randomized	0.4285	<b>0.3424</b>

We measure the main causes of multifractality of two series pairs through the ranges of the multifractal spectra of original, shuffled, and phase-randomized series. As shown in Table 5, we summarize the strength of multifractality for the original, shuffled and phase-randomized series using MF-DCCA. The bold values indicate the significance of multifractality. The results show that large part of the multifractalities are removed by phase randomizing the original series pairs. The results refer that the fat-tailed distributions are the main causes of multifractal features for the two time series pairs.

### 5. Conclusions

In this article, we investigated the relations between respirable particulate  $PM_{10}$  and human respiratory diseases. Firstly, cross-correlation test was conducted and the results show the long-range cross-correlations between  $PM_{10}$  concentration and respiratory diseases time series. Then we applied DCCA coefficient test to further confirm the conclusion, we consisted series pairs from any two time series by  $PM_{10}$ , bronchitis, and rhinitis time series. we found the cross-correlations of Bronchitis/Rhinitis is the largest, then the  $PM_{10}$ /Bronchitis, afterwards the  $PM_{10}$ /Rhinitis. To study from the perspective of multifractality and quantity, we used MF-DCCA to investigate the multifractality of  $PM_{10}$ /Bronchitis, and  $PM_{10}$ /Rhinitis time series pairs. At first, three separate time series such as the monthly average concentration of  $PM_{10}$ , the monthly average outpatient quantity of bronchitis, and the monthly average outpatient quantity of rhinitis time series are analyzed by MF-DFA. We noticed the long-range correlations exist in all the three time series, and the multifractality of all the time series are strong. Then we used MF-DCCA to investigate the cross-correlations between respiratory diseases and  $PM_{10}$  time series pairs. We found that the multifractal properties are significant. Besides, by comparing the degrees of multifractal spectrums, we observed that both the

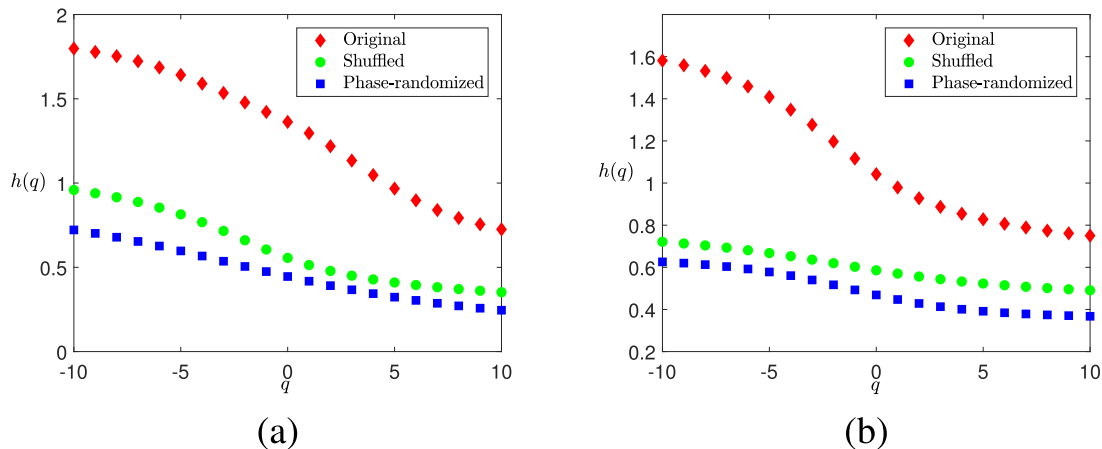
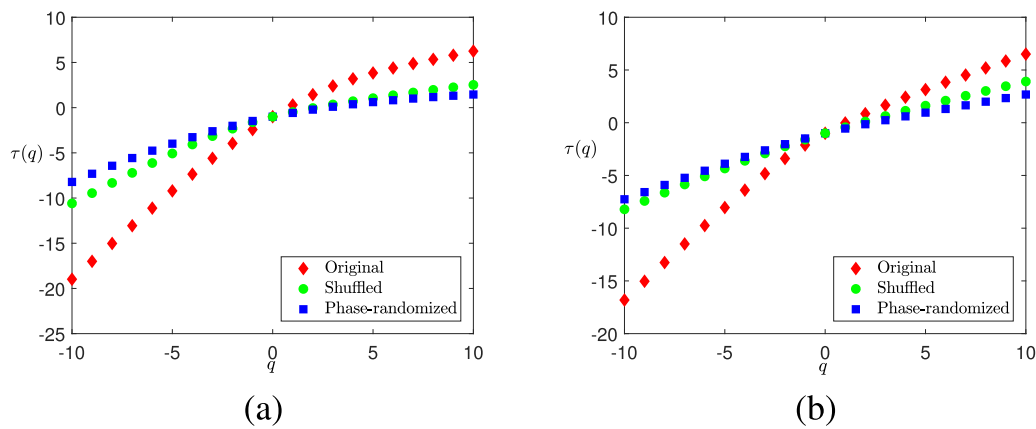
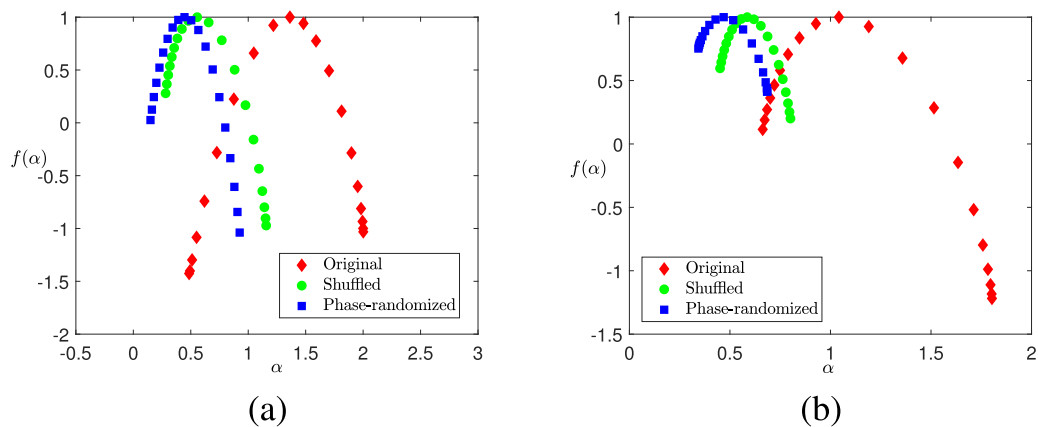


Fig. 12. Generalized Hurst exponents of original, shuffled, and phase-randomized time series of (a)  $PM_{10}$ /Bronchitis, and (b)  $PM_{10}$ /Rhinitis. A color version of the figure is available in the web version of the article.



**Fig. 13.** Scaling exponents of original, shuffled, and phase-randomized time series of (a)  $PM_{10}$ /Bronchitis, and (b)  $PM_{10}$ /Rhinitis. A color version of the figure is available in the web version of the article.



**Fig. 14.** Multifractal spectrums of original, shuffled, and phase-randomized time series of  $PM_{10}$ /Bronchitis, and (b)  $PM_{10}$ /Rhinitis. A color version of the figure is available in the web version of the article.

two monthly outpatient volume of respiratory diseases are sensitive to  $PM_{10}$  concentration. The multifractality of the time series pair  $PM_{10}$ /Bronchitis is stronger than that of  $PM_{10}$ /Rhinitis, which indicated that the monthly outpatient volume of bronchitis is more relevance to  $PM_{10}$  concentration. Besides, we shuffled and phase-randomized the original series to explore the major source of multifractality. The results from MF-DCCA algorithm showed that the fat-tailed distributions contribute to the multifractality for cross-correlation between respiratory diseases and  $PM_{10}$  time series pairs. In addition, we believe that our conclusions can provide advice for disease diagnosis and environmental governance. For physicians, they can diagnose the disease from many factors such as congenital or air pollution factors or other causes. For the government, officials can formulate relevant measures such as atmosphere pollution prevention and control laws to reduce the emission of particulate matter, so as to reduce the incidence of respiratory diseases. However, as we know, there are many other pollutants in the atmosphere, such as  $PM_{2.5}$ , sulfide, nitride, ozone, etc. In the current study, we only investigated human respiratory diseases with  $PM_{10}$ , the effects of other factors on bronchitis and rhinitis also need to be studied, and these will be investigated in our future work.

#### Declaration of Competing Interest

We declare that we do not have any commercial or associative interest that represents a conflict of interest in connection with the work submitted.

#### CRediT authorship contribution statement

**Jian Wang:** Methodology, Resources, Writing - review & editing. **Wei Shao:** Data curation, Formal analysis, Writing - review & editing. **Junseok Kim:** Supervision, Writing - review & editing.

#### Acknowledgment

The first author (Jian Wang) was supported by the [China Scholarship Council \(201808260026\)](#). The corresponding author (J.S. Kim) expresses thanks for the support from the BK21 PLUS program. The authors thank the reviewers for their constructive and helpful comments during the revision of this article.

#### References

- [1] Analitis A, Katsouyanni K, Dimakopoulou K, Samoli E, Nikoloulopoulos AK, Petasakis Y, Forastiere F. Short-term effects of ambient particles on cardiovascular and respiratory mortality. *Epidemiology* 2006;17(2):230–3.
- [2] Li D, Li Y, Li G, Zhang Y, Li J, Chen H. Fluorescent reconstitution on deposition of  $PM_{2.5}$  in lung and extrapulmonary organs. *Proc Natl Acad Sci* 2019;116(7):2488–93.
- [3] Pope CA, Burnett RT, Thurston GD, Thun MJ, Calle EE, Krewski D, Godleski JJ. Cardiovascular mortality and long-term exposure to particulate air pollution. *Circulation* 2004;109(1):71–7.
- [4] Atkinson RW, Kang S, Anderson HR, Mills IC, Walton HA. Epidemiological time series studies of  $PM_{2.5}$  and daily mortality and hospital admissions: a systematic review and meta-analysis. *Thorax* 2014;6(7):660–5.
- [5] Kwon HJ, Cho SH, Lagarde F, Pershagen G. Effects of the asian dust events on daily mortality in seoul. *Korea Environ Res Sect A* 2002;90:1–5.
- [6] Jun T, Min IS. Air pollution, respiratory illness and behavioral adaptation: evidence from south korea. *PLoS ONE* 2019;14(8).

- [7] Kim D, Kim J, Jeong J, Choi M. Estimation of health benefits from air quality improvement using the MODIS AOD dataset in seoul. *Korea Environ Res* 2019;173:452–61.
- [8] Zhou WX. Multifractal detrended cross-correlation analysis for two nonstationary signals. *Phys Rev E* 2008;77:066211–1–4.
- [9] Lahmiri S, Bekiros S. Big data analytics using multi-fractal wavelet leaders in high-frequency bitcoin markets. *Chaos Soliton Fract* 2019:109472.
- [10] Ruan Q, Yang H, Lv D, Zhang S. Cross-correlations between individual investor sentiment and chinese stock market return: new perspective based on MF-DCCA. *Physica A* 2018;503:243–56.
- [11] Lahmiri S, Bekiros S. Nonlinear analysis of casablanca stock exchange, dow jones and s&p500 industrial sectors with a comparison. *Physica A* 2020;539:122923.
- [12] Xu N, Shang PJ, Kama S. Modeling traffic flow correlation using DFA and DCCA. *Nonlinear Dyn* 2010;61:207–16.
- [13] Zhang C, Ni Z, Ni L. Multifractal detrended cross-correlation analysis between PM<sub>2.5</sub> and meteorological factors. *Physica A* 2015;438:114–23.
- [14] Wang J, Shao W, Kim J. Cross-correlations between bacterial foodborne diseases and meteorological factors based on MF-DCCA: a case in south korea. *Fractals* 2020.
- [15] Kantelhardt JW, Zschiegner SA, Koscielny-Bunde E. Multifractal detrended fluctuation analysis of nonstationary time series. *Physica A* 2002;316:87–114.
- [16] Lahmiri S, Bekiros S, Avdoulas C. Time-dependent complexity measurement of causality in international equity markets: a spatial approach. *Chaos Soliton Fract* 2018;116:215–19.
- [17] Baranowski P, Gos M, Krzyszczyk J, Siwek K, Kieliszek A, Tkaczyk P. Multifractality of meteorological time series for poland on the base of MERRA-2 data. *Chaos Soliton Fract* 2019;127:318–33.
- [18] Lahmiri S. Generalized hurst exponent estimates differentiate EEG signals of healthy and epileptic patients. *Physica A* 2018;490:378–85.
- [19] Smitha B, Paul JK. Fractal and multifractal analysis of atherosclerotic plaque in ultrasound images of the carotid artery. *Chaos Soliton Fract* 2019;123:91–100.
- [20] Lahmiri S, Chaos BS. Randomness and multi-fractality in bitcoin market. *Chaos Soliton Fract* 2018;106:28–34.
- [21] Menceur M, Mabrouk AB. A joint multifractal analysis of vector valued non gibbs measures. *Chaos Soliton Fract* 2019;126:203–17.
- [22] Lahmiri S, Bekiros S, Salvi A. Long-range memory, distributional variation and randomness of bitcoin volatility. *Chaos Solitons Fract* 2018;107:43–8.
- [23] Podobnik B, Stanley HE. Detrended cross-correlation analysis: a new method for analyzing two non-stationary time series. *Phys Rev Lett* 2008;100:084102.
- [24] Zunino L, Tabak BM, Figliola A, Prez DG, Garavaglia M, Rosso OA. A multifractal approach for stock market inefficiency. *Physica A* 2008;387:6558–66.
- [25] EAF I. Introduction to multifractal detrended fluctuation analysis in matlab. *Fractal Anal Stat Methodol Innovations Best Pract* 2012:97.
- [26] Shen CH, Huang Y, Yan YN. An analysis of multifractal characteristics of API time series in nanjing. *China Physica A* 2016;451:171–9.
- [27] Wang Q. Multifractal characterization of air polluted time series in china. *Physica A* 2019;514:167–80.
- [28] Lashermes B, Abry P, Chainais P. New insights into the estimation of scaling exponents. *Int J Wavelets Multiresolut Inf Process* 2004;2:497–523.
- [29] Ivanov PC, LAN A, Goldberger AL, Havlin S, Rosenblum MG, Struzik ZR, Stanley HE. Multifractality in human heartbeat dynamics. *Nature* 1999;399:461–5.
- [30] Zebende GF. DCCA Cross-correlation coefficient: quantifying level of cross-correlation. *Physica A* 2011;390:614–18.
- [31] Podobnik B, Jiang ZQ, Zhou WX, Stanley HE. Statistical tests for power-law cross-correlated processes. *Phys Rev E* 2011;84:066118.
- [32] Li Z, Lu X. Cross-correlations between agricultural commodity futures markets in the US and china. *Physica A* 2012;391:3930–41.
- [33] Matia K, Ashkenazy Y, Stanley HE. Multifractal properties of price fluctuations of stocks and commodities. *Europhys Lett* 2003;61:422–8.